Ceramics-Silikáty 66 (4), 453-461 (2022)
www.ceramics-silikaty.cz doi: 10.13168/cs.2022.0041

DEGRADATION OF A SULFOCALCIC BINDER IN A MIXTURE WITH CEMENT DUE TO FREEZING AND THAWING

#KLÁRA PULCOVÁ*, MARTINA ŠÍDLOVÁ*, ROSTISLAV ŠULC**, MARTINA KOHOUTKOVÁ***

*Department of Glass and Ceramics, Faculty of Chemical Technology, University of Chemistry and Technology, Prague, Technická 5, 166 28 Prague, Czech Republic
**Department of Construction Technology, Faculty of Civil Engineering, Czech Technical University (CTU), Technická 2, 166 27 Prague, Czech Republic
***Central laboratories, University of Chemistry and Technology, Prague, Technická 5, 166 28 Prague, Czech Republic

#E-mail: klara.pulcova@vscht.cz

Submitted June 15, 2022; accepted August 12, 2022

Keywords: Sulfocalcic Binder, FBC ash, Freeze-Thaw, Corrosion, Porosity, Ettringite

The paper deals with the freeze-thaw (F-T) resistance of pastes prepared from a mixture of Portland cement (CEM) and a new clinker-free calcium sulfate binder (SCB) based on sulfocalcic fly ash (FBC ash). Pastes with varying ratios of these two binders were prepared and their F-T corrosion resistance in water and a 3 % NaCl solution was investigated. Furthermore, the paste aeration effect on the F-T resistance and the change in the phase composition of the paste during F-T cycling was studied. The results showed that the F-T resistance of the CEM-SCB mixtures was higher compared to the pastes prepared from the unmixed binders alone. All the mixed CEM-SCB pastes showed an undisturbed or slightly disturbed surface in both the water and 3 % NaCl environments, i.e., excellent F-T corrosion resistance after 100 and 200 F-T cycles in an environmental test chamber. A change in the ettringite content over time was observed.

INTRODUCTION

The F-T resistance of concrete is especially important in areas where temperatures change below the freezing point due to seasonal variations. If water-soaked concrete is exposed to low temperatures, water converts to ice, which expands the volume by about 9 % [1]. The formation of ice in the concrete causes unfavourable internal hydraulic and osmotic pressures resulting in cracks. The number of cracks and their size increases with time. This is a phenomenon of physical corrosion that occurs during F-T cycles and is often associated with the effect of chemical de-icing agents, which are commonly used as sanding salts in the treatment of roads [2-5].

Moreover, additional osmotic pressures increase during freezing if the system is saturated with salts. This originates in the increase in concentration differences of the salt ions in various areas of the concrete and the diffusion caused by this. The contribution of the osmotic pressure becomes all the more significant if it exceeds the gradient of the solute concentration in the pore [1, 6]. As a result of the combination of frost and salt, there is an increased degree of concrete corrosion by surface damage mechanisms (D-line cracking, pop-out, delamination and scaling) [3], which further accelerates the penetration of the corrosive medium into the concrete. Prolonged exposure also leads to the leaching of the primary binder phases of concrete and the formation of soluble corrosion products, which causes a gradual softening of the cement matrix leading to the complete degradation of the concrete [3, 4].

One of the factors that can improve the resistance of concrete to the F-T is an appropriate porosity adjustment by adding the optimum amount of an aerating additive. The aerating additive creates spherical pores of a specific size, thereby disrupting the network of capillary pores naturally occurring in the concrete. Thus, it reduces its permeability and increases the resistance to the F-T. Although highly permeable concrete is considered to be problematic in terms of corrosion penetration, it is interesting that, with an artificial increase in the porosity, the concrete often shows good results against F-T corrosion, even in the case of normally less F-T resistant concrete containing fly ash [7], [8]. With many studies having addressed the issue of the relationship between the aeration of concrete and F-T, it can generally be concluded that 4–7 % air content is the optimal amount to improve the F-T resistance in water and de-icing agents [3, 9, 10]. This is due to the fact that the pores in the not fully saturated concrete provide space for ice expansion, making them a kind of safety expansion valve for the concrete [3]. Furthermore, there

is a theory that the additive-formed matrix of evenly distributed small pores not only creates protective safety zones for expansion, but also reduces the permeability of the concrete to corrosive substances in general by increasing the cohesiveness of the mixture [3, 9].

Another key factor influencing the F-T resistance of the concrete is the binder composition. As cement is now considered to have a high-carbon footprint, there is an effort to add or replace additives to reduce the environmental burden. Industrial waste and energy by-products (CCPs), such as fly ash, blast furnace granulated slag or silica fume with suitable properties have been used for these proposes [11-12]. The need for the partial or complete replacement of the clinker by CCPs is growing nowadays not only for environmental, but for social and economic reasons above all.

Fly ash is commonly used as an admixture to Ordinary Portland cement to prepare blended cements or concretes. On the other hand, FBC ash, which is formed during fluidised bed combustion and is very often accompanied by dry flue gas desulfurisation, must not be used in concretes due to the high content of free lime and anhydrite (the active CaO must not exceed 10 wt. % ash content, the SO_3 content must not exceed 3 wt. % of the ash content) [13]. In addition, due to the aforementioned high content of free lime and sulfates, FBC ash-based binders exhibit an increased tendency to form undesirable expansion due the secondary ettringite ($3CaO{\cdot}Al_2O_3{\cdot}3CaSO_4{\cdot}32H_2O$) formation, as described by Stark and Bollmann [14] and confirmed by Škvára et al. [15] and Althoey [16]. The expansion can be accelerated in the presence of chlorides via Friedel's salts ($3CaO{\cdot}Al_2O_3{\cdot}CaCl_2{\cdot}10H_2O$) and Kuzel's ($3CaO{\cdot}Al_2O_3{\cdot}½CaSO_4{\cdot}½CaCl_2{\cdot}10H_2O$) salts, as reported by Glasser et al. [17].

Nevertheless, there is a strong tendency to find the use of these CCPs in construction. For this, it becomes imperative to analyse the origin of the CCP and the number of possible expansion products in order to determine the concrete's stability and high F-T strength.

Very little work on this topic has been published regarding the F-T resistance of concretes with a high content of FBC ash (both FBC ash to cement and FBC ash-based binders). However, in the existing literature, the results vary considerably. In some cases, a decrease in the F-T resistance with an increasing FBC ash content has been described [18-20]. On the contrary, Šídlová et al. found that the FBC ash-based binder has a comparable or even higher F-T resistance compared to the reference cement [21]. Based on these results, it may be concluded that the resistance depends on the specific ash or binder from which the mixtures are prepared.

The clinker-free binder SCB based on the FBC ash used in this work is volume-stable with high resistance to salt solutions and demonstrates long-term stable compressive strengths, Škvára et al. [22]. The SCB predominantly contains ground FBC ash and at least 8 wt. % CaO, 2 wt. % $CaSO_4$ and 5 wt. % aluminosilicates. An important component is a polycarboxylate-based plasticiser with a content of up to 2 wt. % by weight of the FBC ash. The water to binder ratio in the range of 20 – 65 % FBC ash is used to prepare the mixtures [22-23].

This work builds on our previous research [21, 23] in which the SCB pastes or mortars were subjected to an F-T test in water or 3 % NaCl. The results show that the hardened pastes or mortars with suitable plasticisers and air-entraining agents demonstrate similar strengths to the reference Portland cement, but higher resistance to F-T in the water and 3 % NaCl environments [21]. The main aim of this work was to determine the F-T behaviour of CEM-SCB mixtures in various proportions and to obtain additional information about the properties of the SCB. Furthermore, the mineralogical phases during the F-T in the 3 % NaCl solution were determined and compared with the composition of the CEM, SCB and CEM-SCB combinations during the F-T cycling. Emphasis is placed on the amount of corrosion products, especially the secondary expansion ettringite and the phases close to it, as the expansive formation of needle-shape crystals of secondary ettringite is a frequent cause of degradation of concrete if it contains a high amount of sulfates [3, 15].

EXPERIMENTAL

F-T method

The F-T test was performed according to the modified form of the Czech standard ČSN 73 1326 Z1 [24], variant C, i.e., the method of automatic cycling II. As the preparation of the test specimens described in this standard is often criticised for the poor reproducibility of the results (used sleeves leak), a cylindrical sample preparation procedure on the recommendation of Kocáb et al. [25] was used, namely cylindrical tubes which have been found to produce highly reproducible results.

For the preparation of the cylindrical bodies, cut plastic pipes (tubes) with a diameter of 100 mm with an added bottom seal were used. After filling the cylindrical tubes and vibrating them, the surface was levelled (see Figure 1). The prepared samples were placed in a curing chamber with a water-saturated environment. After 28 days of maturation, either tap water or a 3 % NaCl solution was poured onto the surface of the samples to the height of 10 – 20 mm. The samples were covered with aluminium foil and placed in a Memmert CTC 256 automatic environmental test chamber (Memmert GmbH, Germany). After 25, 50, 75, 100 and 200 cycles were completed, the samples were removed from the chamber in order to determine the degree or intensity of the surface corrosion waste

after the F-T tests. After every 25 F-T cycles, the samples were returned to the chamber with the cleaned surface freshly filled with water or the 3 % NaCl solution.

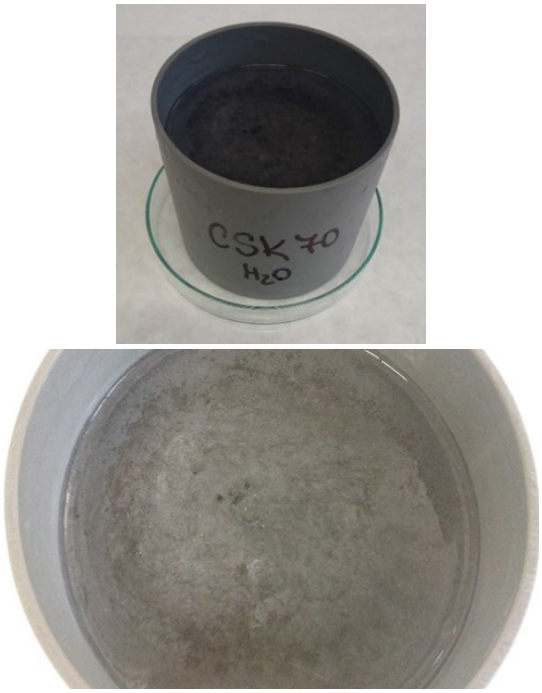

Figure 1. Photo showing the shape and surface of the sample.

The degree of the surface corrosion was evaluated according to the Czech standard ČSN 73 1326 Z1 [24] (Table 1). The limit values of the F-T surface waste were assessed according to the specification of requirements ČSN P 73 2404 [26] for category XF4 – action F-T (concrete highly saturated with water with de-icing agents or seawater – surfaces exposed to direct spray of de-icing agents and frost).

Table 1. Degree of the surface corrosion evaluation, according to the ČSN 73 1326 Z1 standard [24].

Corrosion evaluation	F-T surface waste [g m^{-2}]
1 – Undisturbed	up to 50
2 – Slightly disturbed	50–500
3 – Disturbed	500–1000
4 – Severely disturbed	1000–3000
5 – Crumbled	over 3000

Cubes with an edge of 20 mm were prepared from the same mixtures as the cylindrical samples to study the phase composition. After filling the forms and vibrating them, the surface was levelled and the samples were placed in a curing chamber in a water-saturated environment for 28 days for maturation. Subsequently, the cubes were placed in containers with the 3 % NaCl solution, where they were exposed to the same temperature changes as the cylindrical samples. After the F-T, the cubes were removed from the environment, lightly rinsed with water and subsequently prepared for the X-ray diffraction (XRD) and scanning electron microscope (SEM) analyses

Air content - pressure method

The aeration of the fresh pastes was measured using a pressure apparatus (TESTING Bluhm & Feuerherdt GmbH, Germany) with a volume of 1000 ml. The test was performed according to the standard EN 12350-7 [27]. In order to achieve the optimal aeration, a variant of vibration compaction using a vibrating table was used. The total vibration time was around 2 minutes. This time was chosen as optimal in order to avoid any excessive loss of aeration and to properly prepare the compacted paste.

Other methods

The X-ray diffraction analysis (XRD) was performed at room temperature using a PAN-analytical X'Pert3 Powder θ-θ powder diffractometer (PANalytical, The Netherlands). The qualitative and quantitative analyses were then performed in the HighScore Plus 4.0 software. The amorphous content was determined by an indirect method using an internal standard (10 wt. % ZnO) [28]. The analysis of the phase composition was evaluated using the Rietveld method.

An ARL 9400 sequential wave-dispersive X-ray spectrometer (Thermo, Switzerland) was used to perform the X-ray fluorescence analysis (XRF). The obtained intensities were processed using the Uniquant 4 software without the need to measure the standards. The measurements were made from whole cubes after the F-T.

A Bettersizer ST laser granulometer (Dandong Bettersize Instruments Ltd., China) was used to determine the particle size distribution (PSD) of the binders.

The morphology of the selected hydrated pastes after 100 F-T cycles was monitored by scanning electron microscope (SEM) with Energy-dispersive X-ray spectroscopy (EDX) on a Hitachi S 4700 device (Hitachi, Japan). The EDX analysis was measured from the surface of the cube samples after 100 F-T cycles.

Materials

Portland cement (CEM I 42.5 R) from the Mokrá cement plant (Czech Republic) and the SCB were used for the preparation of the mixtures. The oxide and phase composition are depicted in Tables 2 and 3. The granulometry is plotted using the distribution and cumulative particle distribution curves in Figure 2. Room temperature tap water, air-entraining agent MasterAir 178 (AA) and polycarboxylate superplasticiser (SP) were used.

Table 2. Chemical composition of the SCB and CEM, determined by XRF (wt. %), (LOI = loss on ignition).

XRF	SiO_2	Al_2O_3	CaO	SO_3	Fe_2O_3	TiO_2	MgO	others	LOI
SCB	31.6	24.9	20.2	8.4	4.3	2.3	0.7	1.1	6.5
CEM	18.0	4.6	62.8	4.5	3.4	0.3	1.3	1.7	3.4

Table 3. Phase composition of the SCB and CEM, determined by XRD (wt. %), (Rw = measurement error)

XRD	amorph. phase	anhydrite	quartz	lime	portlandite	calcite	anatase	magnetite	others	Rw
SCB	58.0	15.5	8.5	6.0	5.5	1.5	1.5	1.0	2.5	3.6

XRD	amorph. phase	hatrurite	Larnite	Ca_2FeAlO_5	$Ca_3Al_2O_6$	gypsum	portlandite	others	Rw
CEM	10.0	55.5	17.0	11.0	2.5	2.0	1.5	0.5	8.4

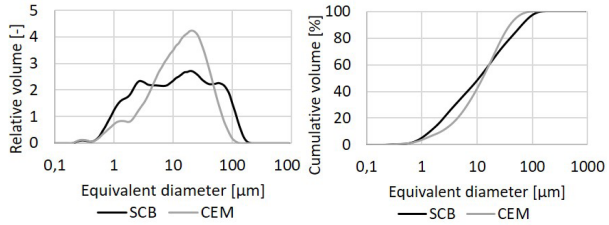

a) frequency curves b) cumulative curves

Figure 2. PSD (µm) of the SCB and CEM.

Preparation of the mixtures

Nine pastes labelled "CSK" (Table 4) were prepared with different CEM to SCB ratios. Two sample equivalents were made from each paste – first for the water resistance testing and second for the 3 % NaCl solution resistance testing. During mixing, the amount of water was optimised to achieve the optimal consistency depending on the to desire optimal aeration about 7 %. The pressure measuring method according to EN 12350-7 [27] was used. The water to binder ratio ranged from 0.19 to 0.29. In addition, two variants of the pastes with 50 % CEM and 50 % SCB with lower (2 %) and higher (13 %) aeration were prepared (Table 4 – CSK 50 2 % and CSK 50 13 %).

RESULTS AND DISCUSSION

F-T results

Figures 3 – 6 show the cumulative amount of the surface waste after the F-T cycling. The values were recorded after 25 F-T cycles. In addition, the graphs show the boundaries referring to the degree of the surface corrosion (Table 1).

It was found (Figure 3) that all the mixed CEM-SCB hardened pastes (CSK 10 – CSK 70) demonstrated significantly higher resistance to the F-T in the water environment compared to the pure CEM (CSK 0) and pure SCB (CSK 100). The mixed CEM-SCB pastes exhibited an undisturbed surface after 100 cycles in the test chamber as well as an undisturbed surface after 200 cycles except for CSK 70 with a value of 76 $g \cdot m^{-2}$, slightly exceeding the limit value of 50 $g \cdot m^{-2}$. The CSK 20 and CSK 50 mixtures had no surface waste after 100 cycles. CSK 0 showed a slightly disturbed surface after 100 and 200 cycles. For CSK 100, the highest degree of degradation was determined after 200 cycles. The higher degradation of the CSK 100 hardened paste was probably caused by a higher water to binder ratio (w = 0.29) compared to the other mixtures with a lower water to binder ratio value, as it is accepted that with a higher water to binder ratio in the paste, its porosity and, thus, susceptibility to the F-T corrosion rises [4].

Compared to the water environment, a higher degradation was observed in all the cycled mixtures in the 3 % NaCl environment (Figure 4). In the NaCl environment, a higher F-T resistance was also observed for the CEM-SCB mixtures, similar to the water environment. These mixed samples showed an undisturbed surface up to 100 cycles, except for the CSK 70 paste, which showed a slightly disturbed surface with a quantity of surface waste of 209 $g \cdot m^{-2}$ after 100 cycles. With further cycling, the amount of the surface waste in the mixtures slightly increased. CSK 100 with a sur-

Table 4. Final composition of the mixtures after the aeration optimisation, (w = water to binder ratio).

Mixture	CEM (g)	CEM (%)	SCB (g)	SCB (%)	w (-)	SP (wt. %)	AA (wt. %)
CSK 0	2000	100	0	0	0.19	2	0.025
CSK 10	1800	90	200	10	0.20	2	0.025
CSK 20	1600	80	400	20	0.20	2	0.025
CSK 30	1400	70	600	30	0.22	2	0.025
CSK 50 2 %	1000	50	1000	50	0.23	2	0.000
CSK 50	1000	50	1000	50	0.23	2	0.025
CSK 50 13 %	1000	50	1000	50	0.23	2	0.050
CSK 70	600	30	1400	70	0.25	2	0.025
CSK 100	0	0	2000	100	0.29	2	0.025

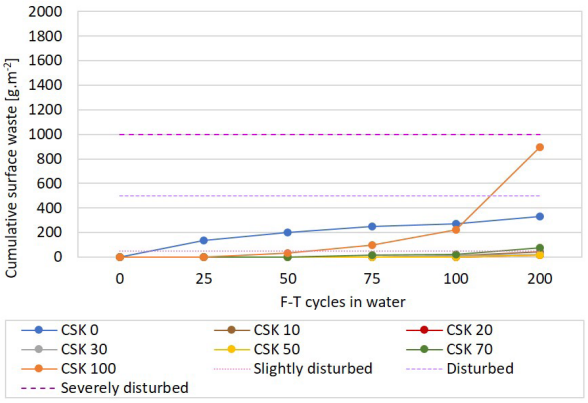

Figure 3. Cumulative amount of the F-T surface waste for the optimally aerated mixtures, CSK 0 – CSK 100, in the water environment.

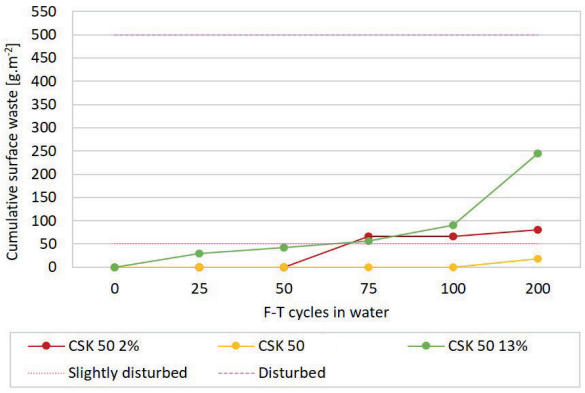

Figure 5. Cumulative amount of the F-T surface waste for the variously aerated CSK 50 mixtures in the water environment.

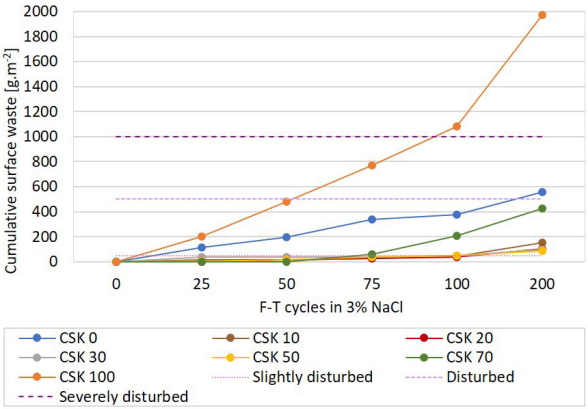

Figure 4. Cumulative amount of the F-T surface waste for the optimally aerated mixtures, CSK 0 – CSK 100, in the 3 % NaCl environment.

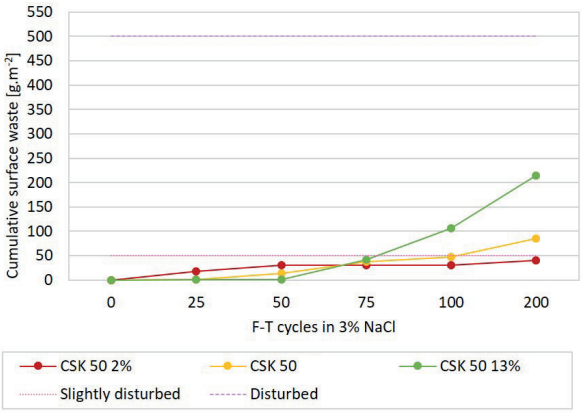

Figure 6. Cumulative amount of the F-T surface waste for the variously aerated CSK 50 mixtures in the 3 % NaCl environment.

face waste of 1083 g·m^{-2} after 100 cycles exceeded the limit of the surface to the area of strongly disturbed. The higher degradation of the sample made from the pure SCB was probably caused by the higher water to binder ratio compared to the other mixtures.

The samples were prepared with different amounts of AA in order to study the possible effect of the aeration on the F-T resistance. It can be seen (Figure 5) that the resistance to the F-T in the water environment for the variously aerated mixtures containing 50 % CEM and 50 % SCB was the highest after 100 cycles for the optimally aerated CSK 50 (aeration 7 %) mixture, which showed an undisturbed surface. The mixtures CSK 50 2 % and CSK 50 13 % had a small amount of surface waste after 100 cycles. During further cycling (up to 200 cycles), a higher tendency to increase the surface waste was evident in the paste with 13 % aeration. The results correspond to the findings reported in the literature [3], where a higher F-T degradation was noted for non-optimally aerated concrete.

Mixtures of various aerations containing 50 % CEM and 50 % SCB were also tested in the 3 % NaCl (Figure 6), with similar resistance results as in the water environment. The effect of the aeration plays a more important role than the influence of the environment type. The CSK 50 2 % and CSK 50 mixtures had a similar amount of surface waste after 100 cycles corresponding to the undisturbed surface. Subsequently, after 200 cycles, the amount of surface waste increased slightly. For the most aerated paste, CSK 50 13 %, after 100 and 200 cycles, the surface degradation was, again, the highest (as in the water environment), although only a slightly damaged surface was recorded.

Once all the obtained F-T results have been compared, it is evident that the resistance of the CEM-SCB mixtures (CSK 10 – CSK 70) decreased only slightly with the increasing F-T cycles, compared to the pure SCB and pure CEM, for which the surface degradation rate was considerably higher. For the optimally aerated mixtures (Figures 3 – 4), there was a noticeable decrease in the resistance in the environment of the 3 % NaCl compared to the water environment. The resistance of the CEM-SCB mixtures was higher in comparison with the binders themselves, as all the CEM-SCB mixed pastes with the optimal aeration (CSK 10 – CSK 70) showed an undisturbed or a slightly disturbed surface

after 100 and 200 cycles in the test chamber in both environments (Table 1). Concerning the specification of the requirements of the standard ČSN P 73 2404 [26] for the XF4 category, the limit corresponding to the C cycling method after 75 F-T cycles, which determines the value of 1000 $g \cdot m^{-2}$ surface waste, has been met.

In contrast to fly ash concrete, which is less resistant to the F-T in NaCl [20], [29], very good F-T resistance was found for the CEM-SCB mixtures, especially for the CSK 50 samples. The higher amount of surface waste in CSK 70 and CSK 100 may be partly related to their higher water to binder ratio. The other mixed pastes showed excellent resistance to the F-T in both environments. The reason for the higher resistance of the mixed pastes with an SCB content of up to 50% by weight is yet to be explained.

From the point of view of the different degrees of aeration (Figure 5 – 6), it was found that the F-T resistance was higher for the samples with the lower and optimal aeration, i.e., 2 – 7 %. These results approximate the values suggested by Verbeck and Klieger [10].

Phase analysis results during F-T

Tables 5 – 7 show the changes in the phase composition during the F-T in the 3 % NaCl environment for the CSK 0, CSK 50 and CSK 100 cube samples. Table 5 shows the phase composition of the CSK 0 sample. CSK 0 contained 59 – 62 % of the amorphous phase, as well as a small proportion of ettringite and hydrated cement characteristic phases such as portlandite, hatrurite, brownmillerite, larnite and calcite. The results showed a slightly increasing content of ettringite with an increase in the number of F-T cycles in the 3 % NaCl, from 4 % before cycling to 7 % after 100 cycles.

Table 6 shows the XRD results of the CSK 100 paste. The hardened paste, again, contained a high proportion of amorphous phase at 64 – 68 %. CSK 100 contained the highest amount of ettringite of all the monitored mixtures. Quartz, anhydrite, calcite and magnetite were found as the minor phases. Anatase was detected as a trace phase. A slight increase in the amount of ettringite during the cycling of the sample in the test chambre is also evident in this case.

Table 7 contains the phases found in the hardened CSK 50 sample, i.e., the sample containing 50 % CEM and 50 % SCB, during cycling. There was a high proportion of the amorphous phase at 61 – 65 %; moreover, ettringite, quartz, anhydrite and phases typical of cement, such as portlandite, hatrurite, calcite, were found. Also trace amounts of phases not listed in the table such as larnite, brownmillerite, magnetite and anatase were observed. In the case of CSK 50, it was noted that the ettringite content increased with any further F-T cycling. Its amount increased from 14 % to 18 % during the cycling at the expense of a decrease in the proportion of the amorphous phase. In the composition of CSK 50, the phases contained in CSK 0 and CSK 100 also appeared, as was expected for the CEM-SCB mixture.

In this section, special attention was paid to the quantity of the expansive ettringite and near-ettringite phases, such as the Friedel and Kuzel salt in the CSK 0, CSK 50, and CSK 100 samples. In contrast to previous research by Šídlová et al. [21], Friedel's salt and Kuzel's salt were not detected by the XRD analysis in this case. The reason for this may be that these phases are formed and disappear in too short of a time interval, which was not possible to capture during the analyses or were below the detection limit of the XRD method. Other compounds containing

Table 5. Phase composition of CSK 0 (wt. %), XRD – Rietveld method.

F-T cycles	amorph. phase	ettringite	portlandite	hatrurite	brownmillerite	larnite	calcite	Rw
0	62	4	9	16	2	2	5	5.8
50	59	6	11	16	2	2	4	6.8
75	59	6	11	15	2	2	5	5.9
100	60	7	10	15	2	2	4	5.5

Table 6. Phase composition of CSK 100 (wt. %), XRD – Rietveld method.

F-T cycles	amorph. phase	ettringite	quartz	anhydrite	calcite	magnetite	Rw
0	68	22	4	2	3	1	4.3
50	64	27	4	2	2	1	4.5
75	65	25	5	2	2	1	4.2
100	64	25	5	2	3	1	4.3

Table 7. Phase composition of CSK 50 (wt. %), XRD – Rietveld method.

F-T cycles	amorph. phase	ettringite	portlandite	quartz	hatrurite	anhydrite	calcite	others	Rw
0	65	14	5	2	7	1	4	2	4.7
50	61	17	5	3	8	1	3	2	4.7
75	63	17	5	2	7	1	3	2	4.5
100	62	18	4	2	7	1	4	2	4.6

chlorides, such as $CaCl_2$ and NaCl, were not detected using the XRD method either. During the F-T test in the 3% NaCl, a very slight increase in the ettringite content was observed in all the pastes compared to the uncycled samples. Although the SCB paste, unlike CEM paste, contains high levels of sulfates, it was found that the amount of ettringite in the SCB samples did not increase significantly during the F-T cycling and the increase in the ettringite during the cycling for CSK 100 (increase of ettringite by 3 %) and CSK 50 (increase of ettringite by 4 %) was comparable to the samples prepared from the CEM alone, i.e., CSK 0 (an increase in the ettringite by 3 %).

SEM after F-T

The following SEM images (Figure 7 – 9) show the surface of the hardened pastes CSK 0, CSK 50 and CSK 100 after the F-T. The images were taken on the cube specimens after 100 F-T cycles in the 3 % NaCl. The EXD analysis of the binder shows that it mainly contains calcium, sulfur, aluminium and silicon. These results are in accordance with the work of Škvára et al., where, in addition to the C-S-H phase, the C-A-S-H phase was detected in the hardened binder from the sulfocalacic fly ash [23].

Specifically, Figure 7 shows portlandite crystals typical of hydrated cement in the CSK 0 sample, in addition, an amorphous binder phase appears there. In Figure 8, containing the images of CSK 100, grown needle-like crystals of ettringite are present together with an amorphous binder phase and a small amount of anhydrite, which corresponds to the XRD analyses. Furthermore, for CSK 100, there are obvious cracks in the material after frost stress, which correspond to the results of the F-T tests, where the smallest resistance to the F-T was found for the CSK 100 sample after 100 cycles in the 3 % NaCl. As for the mixed sample, CSK 50 (Figure 9), the presence of both ettringite crystals and an amorphous binder phase is also evident there. Also, a small amount of deformed portlandite and anhydrite crystals are shown and confirmed by the point EDX analysis.

CONCLUSIONS

The F-T resistance of mixed pastes of the clinker-free binder SCB and CEM was investigated. It was found that the resistance of the CEM-SCB mixtures is higher compared to the CEM paste alone and the SCB paste alone in both the water and 3 % NaCl

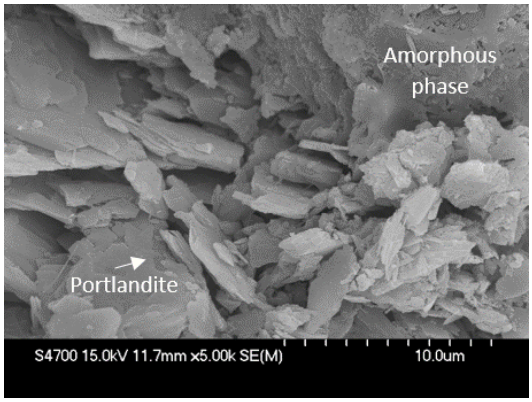

a) 5000 ×

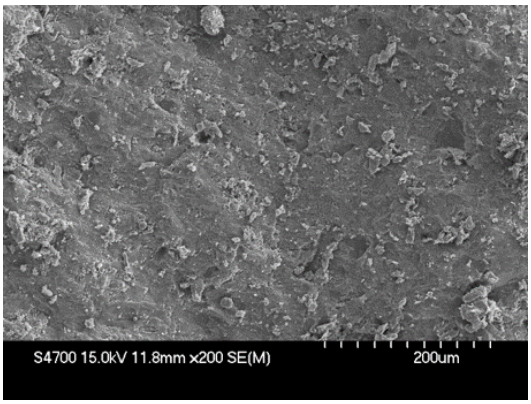

b) 200 ×

Figure 7. (SEM) Surface of the hardened CSK 0 paste after 100 F-T cycles in the 3 % NaCl.

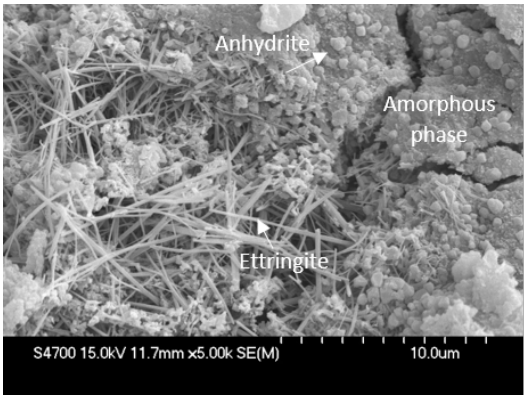

a) 5000 ×

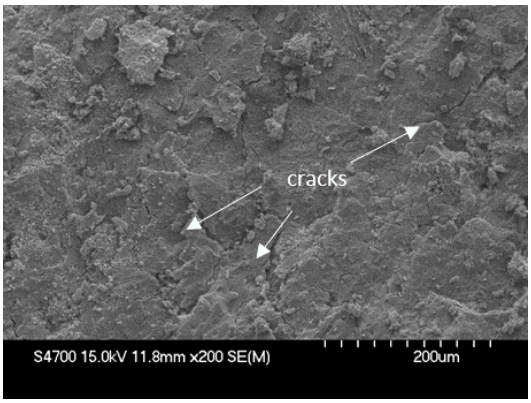

b) 200 ×

Figure 8. (SEM) Surface of the hardened CSK 100 paste after 100 F-T cycles in the 3 % NaCl.

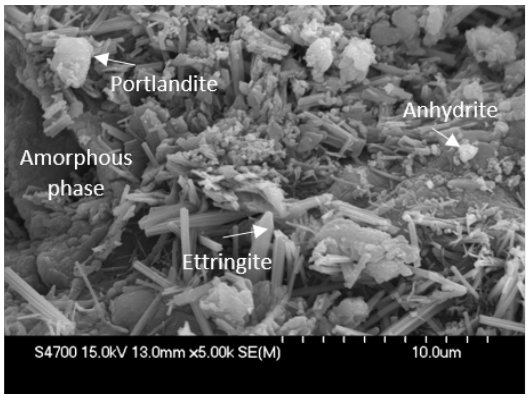

a) 5000 ×

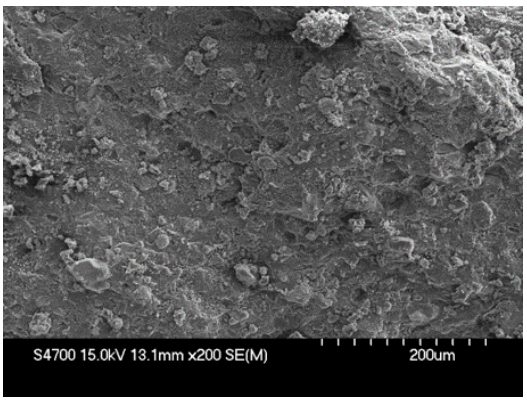

b) 200 ×

Figure 9. (SEM) Surface of the hardened CSK 50 paste after 100 F-T cycles in the 3 % NaCl.

solution environment. The mixed pastes with a content of 10 – 70 % CEM replacement with the SCB showed an undisturbed or a slightly disturbed surface according to the ČSN 73 1326 Z1 standard in both environments after 100 and 200 F-T cycles in the environmental test chamber. This conclusion is significant for using FBC ash binders in practice as they can be applied as an admixture in mixed cements and concretes used in outdoor constructions. However, the higher resistance of the mixed pastes with the SCB content of up to 50 % remains to be explained.

Concerning the aeration, the samples with a lower and optimal aeration were found to withstand the F-T better, i.e., in the range of 2–7 %. Furthermore, it was found that the amount of ettringite in the samples does not significantly increase with the SCB and the values of the increase in the amount of ettringite are comparable to the increase for the pure CEM samples.

Acknowledgments

This work was supported from TAČR FW01010195 – Advanced and innovative processing technologies for strategic utilization and storing of coal combustion products (CCPs); 2020–2023

This work was supported from the grant of Specific university research – grant No A1:FCHT_2022_002.

REFERENCES

1. Neville A. M. (1995). *Properties of Concrete*. 4th ed. Addison Wesley Longman, Harlow.
2. Powers T. C. (1955): *Basic Considerations Pertaining to Freezing and Thawing Tests*. Research Department Bulletin RX058. Portland Cement Association.
3. Page C. L., Page M. M. (2007). *Durability of concrete and cement composites*, 1st ed. Woodhead Publishing Limited.
4. Hewlett P. C., Liska M. (2017). *Lea's Chemistry of Cement and Concrete*. 5th ed. Butterworth-Heinemann. doi:10.1016/C2013-0-19325-7
5. Pigeon M., Pleau R. (1995). *Durability of Concrete in Cold Climates*. E&FN Spon. London. doi:10.1201/9781482271447
6. Powers T. C. (1975): Freezing Effects in Concrete. *ACI American concrete institut*, 47, 1–11.
7. Siddique R., Cachim P. (2018). *Waste and Suplementary Cementitious materials in Concrete*. Woodhead Publishing. doi:10.1016/C2016-0-04037-8
8. Malhotra V. M. (1990): Durability of concrete incorporating high-volume fly ash of low calcium (ASTM Class F) fly ash. *Cement and Concrete Composites*, 12 (4), 271–277. doi:10.1016/0958-9465(90)90006-J
9. Powers T. C. (1949): The air requirement of frost-resistant concrete. *Proc. Highway Research Board, 29*, 184–211.
10. Verbeck K., Klieger P. (1957): Studies of "salt" scaling of concrete. *Portland Cement Association, bulletin 83*.
11. EN 197-1 (2011): Cement Part 1: *Composition, specifications and conformity criteria for common cements*. European Committee for Standardization.
12. EN 206+A2 (2021): *Concrete – Specification, performance, production and conformity*. European Committee for Standardization.
13. EN 450-1 (2012): *Fly ash for concrete – Part 1: Definition, specifications and conformity criteria*, European Committee for Standardization.
14. Stark J., Bollmann K. (1999): Delayed ettringite formation in concrete. *Nordic Concrete Federation, 23*, 10–23.
15. Škvára F., Šulc R., Snop R., Zlámalová-Cílová Z., Peterová A., Kopecký L., Formáček P. (2016): Czech fluid sulfocalcic fly ash. *Ceramics-Silikáty, 60* (4), 344–352. doi:10.13168/cs.2016.0051
16. Althoey F. (2021): Compressive strength reduction of cement pastes exposed to sodium chloride solutions: Secondary ettringite formation. *Construction and Building Materials, 299*, 123965. doi:10.1016/j.conbuildmat.2021.123965
17. Glasser F. P., Kindness A., Stronach S. A. (1999): Stability and solubility relationships in AFm phases Part I. Chloride, sulfate and hydroxide. *Cement and Concrete Research, 29*, 861–866. doi:10.1016/S0008-8846(99)00055-1
18. Naik T. R., Kraus R. N., Chun Y., Botha F. D. (2005): Cast-Concrete Products Made with FBC Ash and Wet-Collected Coal-Ash. *Journal of Materials in Civil Engineering, 17* (6), 659–663. doi:10.1061/(ASCE)0899-1561(2005)17:6(659)
19. Jozwiak-Niedzwiedzka D. (2009): Effect of fluidized bed combustion fly ash on the chloride resistance and scaling resistance of concrete. In: *RILEM Proceedings PRO,Conference Concrete in aggressive aqueous environments - Performance, Testing, and Modeling, 63*, 556–563.
20. Bouzoubaâ N., Bilodeau A., Fournier B., Hooton R. D., Gagné R., Jolin M. (2008): Deicing salt scaling resistance

of concrete incorporating fly ash and (or) silica fume: laboratory and field sidewalk test data. *Canadian Journal of Civil Engineering, 38* (4), 373–382. doi:10.1139/l11-008

21. Šídlová M., Škvára F., Pulcová K., Peterová A., Šulc R., Snop R. (2019): *Resistance of Non-cement Binder to Freezing and Thawing Cycles*. In: EuroCoalAsh 2019 Conference Proceedings, 137–144.
22. VŠCHT v Praze, ČVUT v Praze, ČEZ Energetické produkty, s.r.o. (2020): *A method for producing an ash-based hydraulic binder, a hydraulic binder and their use.* Patent CZ, 308584.
23. Škvára F., Šulc R., Snop R., Peterová A., Šídlová M. (2018): Hydraulic clinkerless binder on the fluid sulfocalcic fly ash basis. *Cement and Concrete Composites, 93*, 118–126. doi:10.1016/j.cemconcomp.2018.06.020
24. ČSN 73 1326 Z1 (2003): *Stanovení odolnosti povrchu cementového betonu proti působení vody a chemických rozmrazovacích látek*. Český normalizační institut.
25. Kocáb D., Misák P., Vymazal T., Komárková T., Halamová R. (2017): Stanovení odolnosti povrchu betonu proti působení vody a chemických rozmrazovacích látek – metody, praxe, problémy. *Časopis Beton, 2*, 42–47.
26. ČSN P 73 2404 (2016): *Beton – Specifikace, vlastnosti, výroba a shoda – Doplňující informace*. Úřad pro technickou normalizaci, metrologii a státní zkušebnictví, Praha.
27. EN 12350-7 (2019): *Testing fresh concrete - Part 7: Air content - Pressure methods*. Czech office for standards, metrology and testing. European Committee for Standardization.
28. Šídlová M., Maixner J., Škvára F., Kohoutková M., Cibulková J., Polonská A. (2019): Characterization of Czech coal combustion ashes and their hydrated products. *Waste Forum, 3*, 276–286.
29. Thomas M. D. A. (2007). *Optimizing the Use of Fly Ash in Concrete*. Portland Cement Association, IS548.